

A41B-0045 : Photolysis frequency and cloud dynamics during DC3 and SEAC4RS

S. R. Hall¹, K. Ullmann¹, S. Madronich¹, J.W. Hair², M.A. Fenn², C.R. Butler²

¹. National Center for Atmospheric Research (NCAR), Boulder, CO ². NASA Langley Research Center, Hampton, VA



Abstract

Cloud shading plays a critical role in extending the lifetime of short-lived chemical species. During convection, photochemistry is reduced and short-lived species may be transported from the boundary layer to the upper troposphere/lower stratosphere (UTLS). In the anvil outflow, shading continues within and below the cloud. However, near the highly scattering cloud top, photochemistry is greatly accelerated. In this rapidly evolving environment, accurate photolysis frequencies are required to study composition evolution. During the Deep Convective Clouds and Chemistry (DC3, 2012) and the Studies of Emissions and Atmospheric Composition, Clouds and Climate Coupling by Regional Surveys (SEAC4RS, 2013) campaigns, photolysis frequencies were calculated from measurements of spectrally resolved actinic flux by the Charge-coupled device Actinic Flux Spectroradiometer (CAFS) on the NASA DC-8 and the HIAPER Airborne Radiation Package (HARP) on the NCAR G-V aircraft. Input of cloud characteristics into the Tropospheric Ultraviolet and Visible (TUV) Radiation model constrained cloud optical depths for spatially and temporally stable conditions. Statistical correlations of the data reveal modal behavior that could help assess cloud fields in global chemistry models.

CAFS/HARP Components

CCD Monochromator

- Hamamatsu S7301-906 windowless back-thinned, blue-enhanced, cooled, 534 pix
- Electronics: tec5 timing, cooling, control, acquisition and spectral averaging to minimize detector and read noise
- Housing: Zeiss monolithic ceramic with epoxy attached slit, grating and CCD for temperature and vibration stability
- Wavelength range: 280-680 nm
- Wavelength resolution: ~1.8 nm FWHM at 297 nm
- Accuracy: 5% in UV-B, 3% in UV-A/VIS limited by NIST standards
- Detection limit: ~0.04 mW/m²/nm at 300 nm
- Precision: 1-2% depending on wavelength

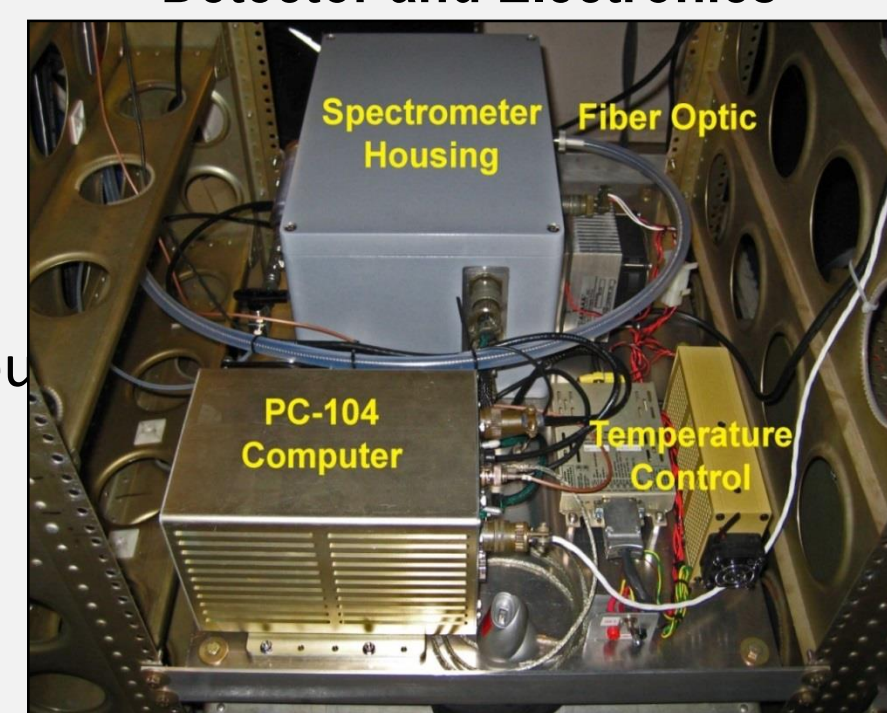
Optical Collector



Data Acquisition

- Small, light, low power PC/104+ computer system
- 16 bit data acquisition
- D/A temperature, pressure and humidity monitoring
- IRIG-B time synchronization
- Custom LabVIEW data acquisition and control software

Detector and Electronics



Quartz optical collectors

- 2π steradian hemispherical optics
- 30 cm artificial horizon

Fiber Optic Bundles

- High OH fused silica for high UV throughput

Detector Specifications

- Mass: 18 kg / instrument
- Power: 2.5 A of 115 VAC
- Rack Height: 20 cm

TUV Radiative Transfer Model

Actinic flux was modeled using a highly modified Tropospheric Ultraviolet and Visible version 4+ using 8-stream discrete ordinate radiative transfer method with a pseudo-spherical modification. The calculation includes absorption by O₂ and O₃, Rayleigh scattering and scattering and absorption by aerosols. Standard model conditions consist of cloud free skies (or cloud layers), vertical profiles of air and temperature from the US Standard Atmosphere, Elterman aerosol profile and total ozone columns from the Ozone Monitoring Instrument (OMI) on the EOS Aura satellite.

The model was run for each minute of measurement using the *in situ* latitude, longitude, altitude, temperature, and pressure and a fixed albedo of 0.04. TUV generated modeled actinic fluxes with a 1 nm wavelength grid from 292-680 nm. Photolysis frequencies were then calculated from the actinic flux:

$$\text{Photolysis Frequency} = \int F(\lambda) \sigma(\lambda, T, p) \phi(\lambda, T, p) d\lambda$$

The CAFS, HARP and TUV spectra were processed using the same j-value calculation code to ensure that the same quantum yield (Φ), absorption cross section (σ), temperature (T) and pressure (p) dependence relationships were applied to both the measured and modeled spectra.

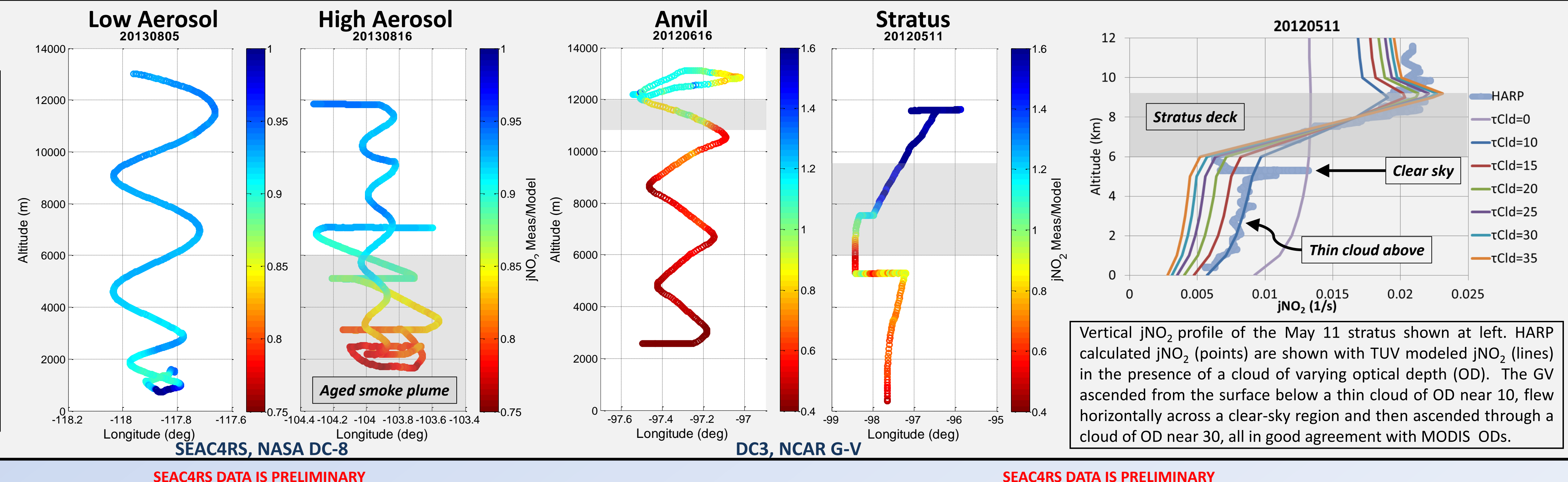
Photolysis Frequencies

- $j[\text{O}_3 \rightarrow \text{O}_2 + \text{O}(^1\text{D})]$
- $j[\text{NO}_2 \rightarrow \text{NO} + \text{O}(^3\text{P})]$
- $j[\text{H}_2\text{O}_2 \rightarrow 2\text{OH}]$
- $j[\text{HNO}_2 \rightarrow \text{OH} + \text{NO}]$
- $j[\text{HNO}_3 \rightarrow \text{OH} + \text{NO}_2]$
- $j[\text{CH}_2\text{O} \rightarrow \text{H} + \text{HCO}]$
- $j[\text{CH}_2\text{O} \rightarrow \text{H}_2 + \text{CO}]$
- $j[\text{CH}_3\text{CHO} \rightarrow \text{CH}_3 + \text{HCO}]$
- $j[\text{CH}_3\text{CHO} \rightarrow \text{CH}_4 + \text{CO}]$
- $j[\text{C}_2\text{H}_5\text{CHO} \rightarrow \text{C}_2\text{H}_5 + \text{HCO}]$
- $j[\text{CHOCHO} \rightarrow \text{products}]$
- $j[\text{CHOCHO} \rightarrow \text{HCO} + \text{HCO}]$
- $j[\text{CH}_3\text{COCHO} \rightarrow \text{products}]$
- $j[\text{CH}_3\text{COCH}_3 \rightarrow \text{CH}_3\text{CO} + \text{CH}_3]$
- $j[\text{CH}_3\text{OOH} \rightarrow \text{CH}_3\text{O} + \text{OH}]$
- $j[\text{CH}_3\text{ONO}_2 \rightarrow \text{CH}_3\text{O} + \text{NO}_2]$
- $j[\text{PAN} \rightarrow \text{products}]$
- $j[\text{CH}_3\text{COCH}_2\text{CH}_3 \rightarrow \text{Products}]$
- $j[\text{CH}_3\text{CH}_2\text{CH}_2\text{CHO} \rightarrow \text{C}_3\text{H}_7 + \text{HCO}]$
- $j[\text{CH}_3\text{CH}_2\text{CH}_2\text{CHO} \rightarrow \text{C}_2\text{H}_4 + \text{CH}_2\text{CHOH}]$
- $j[\text{HO}_2\text{NO}_2 \rightarrow \text{HO}_2 + \text{NO}_2]$
- $j[\text{HO}_2\text{NO}_2 \rightarrow \text{OH} + \text{NO}_3]$
- $j[\text{CH}_3\text{CH}_2\text{ONO}_2 \rightarrow \text{Products}]$
- $j[\text{Br}_2 \rightarrow \text{Br} + \text{Br}]$
- $j[\text{BrO} \rightarrow \text{Br} + \text{O}]$
- $j[\text{Br}_2\text{O} \rightarrow \text{products}]$
- $j[\text{BrNO}_3 \rightarrow \text{Br} + \text{NO}_3]$
- $j[\text{BrNO}_3 \rightarrow \text{BrO} + \text{NO}_2]$
- $j[\text{BrCl} \rightarrow \text{Br} + \text{Cl}]$
- $j[\text{HOBr} \rightarrow \text{HO} + \text{Br}]$
- $j[\text{BrONO}_2 \rightarrow \text{Br} + \text{NO}_3]$
- $j[\text{BrONO}_2 \rightarrow \text{BrO} + \text{NO}_2]$
- $j[\text{Cl}_2 + \text{hv} \rightarrow \text{Cl} + \text{Cl}]$
- $j[\text{ClO} \rightarrow \text{Cl} + \text{O}]$
- $j[\text{ClONO}_2 \rightarrow \text{Cl} + \text{NO}_3]$
- $j[\text{ClONO}_2 \rightarrow \text{ClO} + \text{NO}_2]$

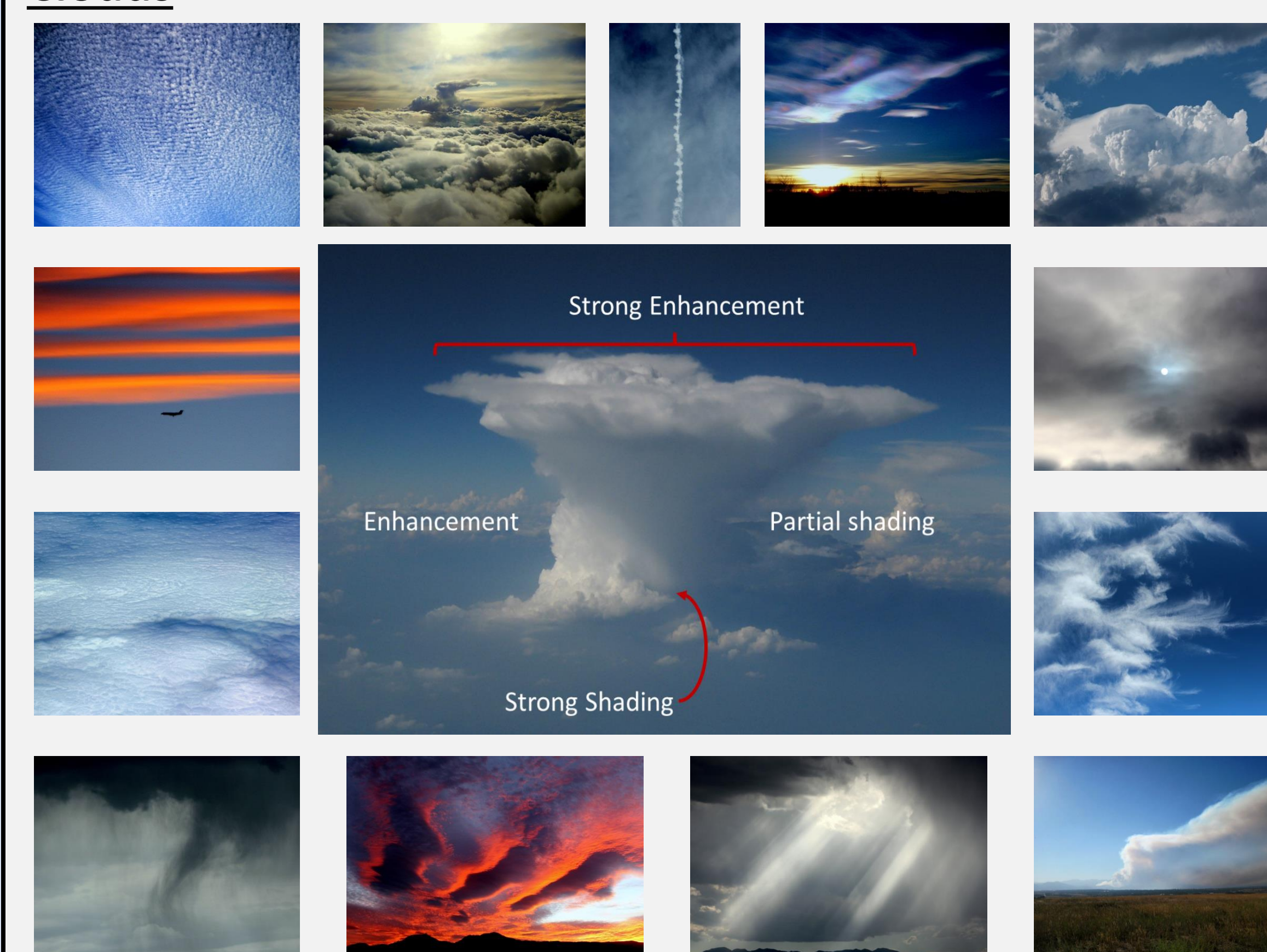
Profiles

Aircraft profiles color coded with the ratio of CAFS/HARP measured $j\text{NO}_2$ to TUV modeled $j\text{NO}_2$ under various cloud and aerosol conditions.

Values less (greater) than one indicate reduced (enhanced) actinic flux due to the cloud and aerosol influence. All cases occurred with overlying clear skies.



Clouds



Clouds and aerosols strongly alter the atmospheric light environment. Statistical data analyses support understanding the variety of shapes, sizes, altitudes, layering, optical depths, microphysical parameters and sensitivity to solar zenith angle.

Discussion

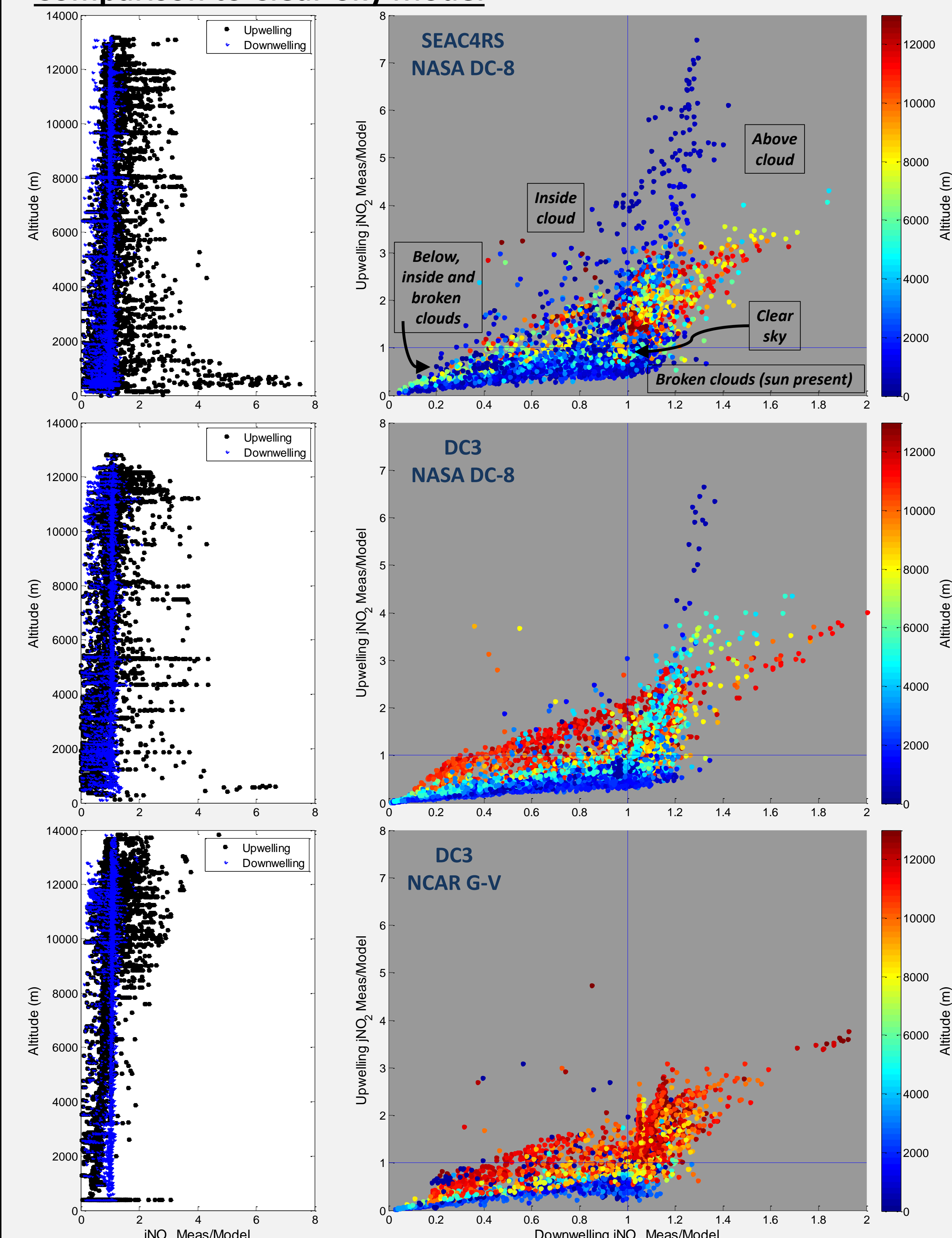
The DC3 and SEAC4RS field projects provided a rich database for study of atmospheric photolysis frequencies in the presence of aerosols and clouds. Profile data demonstrates the strong impact on photolysis frequencies. Optical depth may be estimated from the CAFS/HARP measurements for reasonably stable clouds of wide horizontal extent.

Palancar et al. (ACP, doi:10.5194/acp-11-5457-2011) first revealed a modal behavior in actinic flux by correlating the ratio of measurement to clear-sky model of the separate up and downwelling radiation components during the NASA INTEX-NA campaign. The modes are the result of *in situ* enhancements and reductions of actinic flux by clouds and aerosols. This study encompassing all data from three aircraft deployments indicates an altitude dependence to the correlation.

Further study includes examination of:

- The cause of the **altitude dependence** of up and downwelling radiation components.
- Mission **sampling bias** by analysis of multiple missions under widely variable geographical and meteorological conditions.
- Cloud schemes used in **chemistry transport models** for modal behavior. Do they accurately represent photolysis?
- The **impact of the photochemical environment on redistributed species** due to convection and monsoonal flows and the impacts on the UT/LS, cirrus and cumulus anvil regimes, biomass burning plumes and local air quality.
- Additional case studies to determine **cloud optical depth** and the effects of cloud variability on photochemistry.

Comparison to Clear-Sky Model



CAFS and HARP measure up and downwelling radiation independently. The TUV model also generates these directional components. On the left, the ratio of measured to clear-sky modeled component $j\text{NO}_2$ as a function of altitude is shown for each aircraft deployment. The high altitude bias of the DC3 G-V flights is apparent. On the right, the correlation of the ratios color coded by altitude is shown, with modal behavior apparent within different cloud morphologies.